Magnetic anisotropy basis sets for epitaxial (110) and (111) $REFe_2$ nanofilms

2008 J. Phys.: Condens. Matter 20 285226

(http://iopscience.iop.org/0953-8984/20/28/285226)

J. Phys.: Condens. Matter **20** (2008) 285226 (7pp) doi:10.1088/0953-8984/20/28/285226

Magnetic anisotropy basis sets for epitaxial (110) and (111) $REFe_2$ nanofilms

G J Bowden[1], **K N Martin, A Fox, B D Rainford and P A J de Groot**

School of Physics and Astronomy, University of Southampton, SO17 1BJ, UK

E-mail: gjb@phys.soton.ac.uk

Received 24 April 2008
Published 24 June 2008
Online at stacks.iop.org/JPhysCM/20/285226

Abstract

Magnetic anisotropy basis sets for the cubic Laves phase rare earth intermetallic $REFe_2$ compounds are discussed in some detail. Such compounds can be either free standing, or thin films grown in either (110) or (111) mode using molecular beam epitaxy. For the latter, it is useful to rotate to a new coordinate system where the z-axis coincides with the growth axes of the film. In this paper, three symmetry adapted basis sets are given, for multi-pole moments up to $n = 12$. These sets can be used for free-standing compounds and for (110) and (111) epitaxial films. In addition, the distortion of $REFe_2$ films, grown on sapphire substrates, is also considered. The distortions are different for the (110) and (111) films. Strain-induced harmonic sets are given for both specific and general distortions. Finally, some predictions are made concerning the preferred direction of easy magnetization in (111) molecular beam epitaxy grown $REFe_2$ films.

(Some figures in this article are in colour only in the electronic version)

1. Introduction

In modelling the properties of anisotropic magnetic compounds, a knowledge of the magnetic anisotropy $E_A(\theta, \phi)$ is essential. For cubic compounds, the phenomenological form is often used:

$$E_A(\alpha_x, \alpha_y, \alpha_z) = K_1\left(\alpha_x^2\alpha_y^2 + \alpha_x^2\alpha_z^2 + \alpha_y^2\alpha_z^2\right) + K_2\alpha_x^2\alpha_y^2\alpha_z^2 \quad (1)$$

(e g. Bozorth 1961, Coey and Skomski 1993). Here K_1 and K_2 are temperature dependent anisotropy parameters while α_x, α_y, and α_z are direction cosines, with respect to the cubic axes. In particular, it is easy to show that the relative values of K_1 and K_2 determine the direction of easy magnetization, which can only lie along either a major [001], [011], or [111] cubic axis.

However in Atzmony and Dariel 1976 (herein referred to as A&D), it was shown that equation (1) is deficient for the strongly anisotropic cubic Laves phase $REFe_2$ intermetallic compounds. From numerous ^{57}Fe Mössbauer experiments on mixed $RE(a)_xRE(b)_{1-x}Fe_2$ compounds, A&D obtained spin-orientation diagrams, in essence setting off the anisotropy of one rare earth against another (Atzmony *et al* 1973). In particular, directions of magnetization were found with non-major $[uuv]$ or $[uv0]$ easy axes, in conflict with the predictions of equation (1). Consequently, A&D modified the anisotropy to include a third term:

$$E_A = K_1\left[\alpha_x^2\alpha_y^2 + \alpha_x^2\alpha_z^2 + \alpha_y^2\alpha_z^2\right] + K_2\left[\alpha_x^2\alpha_y^2\alpha_z^2\right] + K_3\left[\alpha_x^4\alpha_y^4 + \alpha_x^4\alpha_z^4 + \alpha_y^4\alpha_z^4\right]. \quad (2)$$

Further, from Mössbauer data and subsequent analysis A&D were able to (i) deduce values for the cubic crystal field parameters B_4 and B_6, for the differing RE^{3+} ions, and (ii) justify the inclusion of K_3, by calculating the free energy of the RE ions for 30 selected angles, followed by a computer fit to equation (2). However they warned that still higher order terms might be necessary.

In 2006, this problem was revisited by Martin *et al*, who showed that (i) the higher order terms alluded to by A&D are important, and (ii) the magneto-crystalline anisotropy of the free-standing $REFe_2$ intermetallic compounds, correct to second order in the modified Callen and Callen (1965), Callen and Shtrikman (1965), Callen and Callen (1966) model of anisotropy (C&C), can be expressed in the multi-polar form:

$$E_A(\theta, \phi) = \tilde{K}_0(T)Y_0^0(\theta, \phi) + \tilde{K}_4(T)\mathbf{Y}_4^C + \tilde{K}_6(T)\mathbf{Y}_6^C + \tilde{K}_8(T)\mathbf{Y}_8^C + \tilde{K}_{10}(T)\mathbf{Y}_{10}^C + \tilde{K}_{12}(T)\mathbf{Y}_{12}^C. \quad (3)$$

In this expression for the anisotropy, the $\tilde{K}_n(T)$ are temperature dependent parameters, while the $\mathbf{Y}_n^C$ are

[1] Author to whom any correspondence should be addressed.

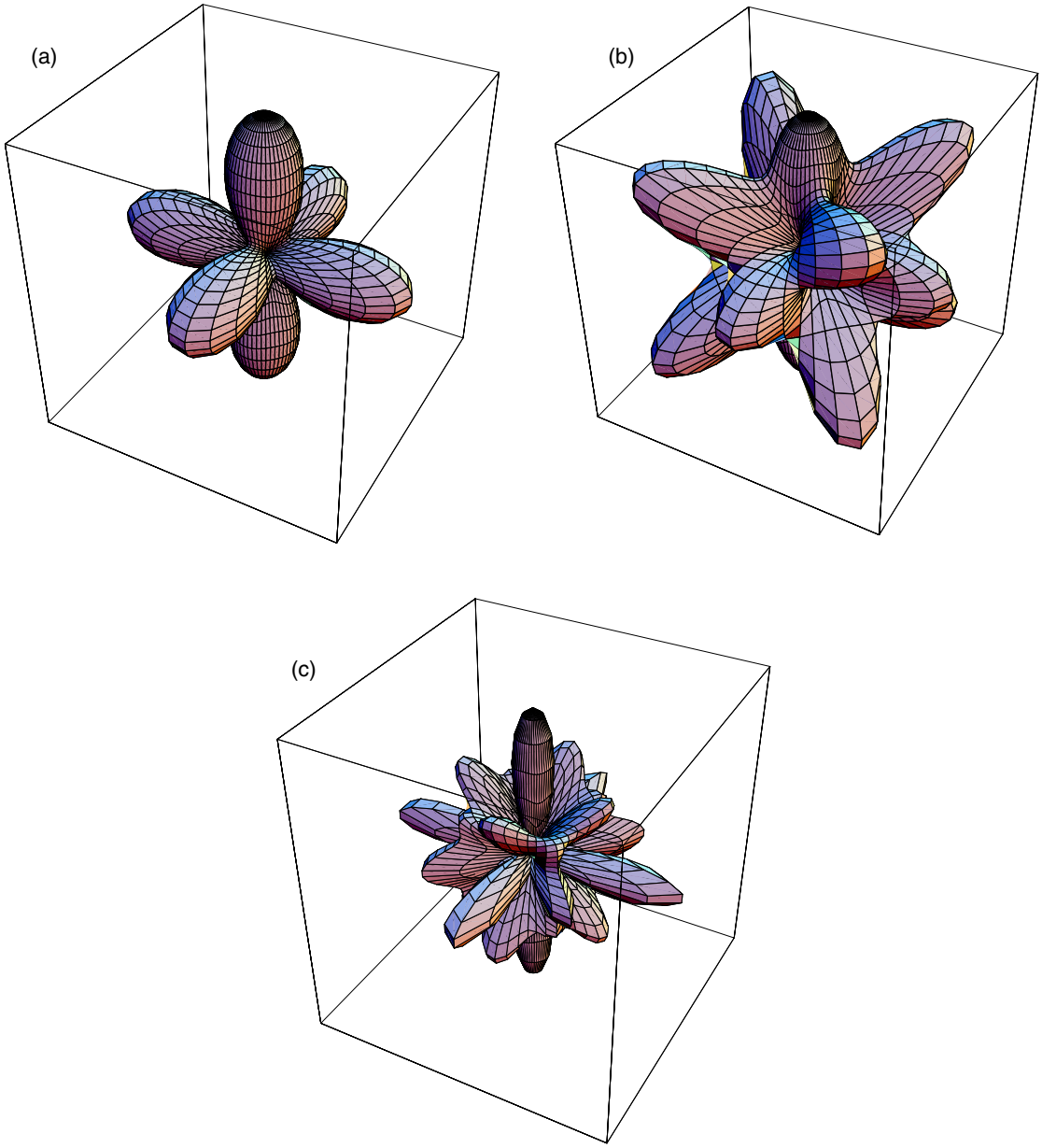

Figure 1. Pictorial representation of the cubic Harmonic $\mathbf{Y}_4^C$ (a) $\mathbf{Y}_6^C$ (b) $\mathbf{Y}_8^C$ (c). A constant has been added to avoid negative lobes.

Table 1a. Combinations of spherical harmonics with cubic symmetry up to rank $N = 12$, after Martin *et al* (2006).

$$\mathbf{Y}_4^C(\theta,\phi) = Y_4^0(\theta,\phi) + \sqrt{\tfrac{5}{14}}(Y_4^4(\theta,\phi) + Y_4^{-4}(\theta,\phi))$$

$$\mathbf{Y}_6^C(\theta,\phi) = Y_6^0(\theta,\phi) - \sqrt{\tfrac{7}{2}}(Y_6^4(\theta,\phi) + Y_6^{-4}(\theta,\phi))$$

$$\mathbf{Y}_8^C(\theta,\phi) = Y_8^0(\theta,\phi) + \tfrac{1}{3}\sqrt{\tfrac{14}{11}}(Y_8^4(\theta,\phi) + Y_8^{-4}(\theta,\phi)) + \tfrac{1}{3}\sqrt{\tfrac{65}{22}}(Y_8^8(\theta,\phi) + Y_8^{-8}(\theta,\phi))$$

$$\mathbf{Y}_{10}^C(\theta,\phi) = Y_{10}^0(\theta,\phi) - \sqrt{\tfrac{66}{65}}(Y_{10}^4(\theta,\phi) + Y_{10}^{-4}(\theta,\phi)) - \sqrt{\tfrac{11\cdot17}{10\cdot13}}(Y_{10}^8(\theta,\phi) + Y_{10}^{-8}(\theta,\phi))$$

$$\mathbf{Y}_{12}^C(\theta,\phi) = Y_{12}^0(\theta,\phi) - \tfrac{4}{9}\sqrt{\tfrac{91}{11}}(Y_{12}^4(\theta,\phi) + Y_{12}^{-4}(\theta,\phi)) + \tfrac{1}{3}\sqrt{\tfrac{13\cdot17\cdot19}{66}}(Y_{12}^8(\theta,\phi) + Y_{12}^{-8}(\theta,\phi))$$

combinations of spherical harmonics with cubic symmetry, listed in table 1a. In essence equation (3) should be viewed as the expansion of the anisotropy energy in terms of a symmetry adapted set $\{\mathbf{Y}_N^C\}$, which form the appropriate angular Fourier components for RE ions with cubic symmetry. The higher the multi-polar order N of the $\mathbf{Y}_N^C$, the more rapid the dependence on the angles (θ, ϕ). This is illustrated in figures 1(a)–(c), for $N = 4$, 6 and 8, respectively. In practice, it is sufficient to terminate the series at $N = 12$ for the $REFe_2$ compounds. Finally, we note that while the $\mathbf{Y}_N^C$ of Martin *et al* (2006) are

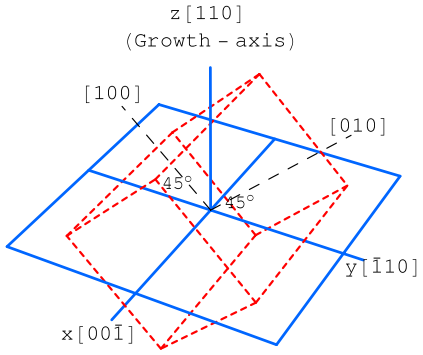

Figure 2. Diagram showing the cubic Laves unit cell (dotted) with respect to the plane of the (110) film. The [$\bar{1}$10] and [00$\bar{1}$] axes are in plane. However the [010] and [100] axes point out of plane at 45° with z-axis, in the z–y plane.

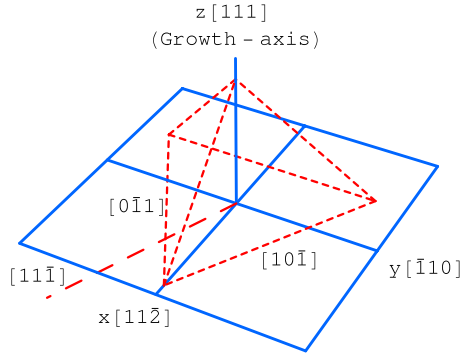

Figure 3. Schematic diagram, showing the corner of the cubic Laves unit cell (dotted) protruding through the plane of the [111] film. The [$\bar{1}$10] and [10$\bar{1}$] and [0$\bar{1}$1] axes are all in plane, making an angle of 120° with respect to each other. Note the presence of the out of plane [11$\bar{1}$] axis, in the z–x plane, at an angle of 71° with the z-axis. This direction plays an important role in the exchange spring driven spin-flop (Martin *et al* 2008).

Table 1b. Normalized combinations of spherical harmonics with cubic symmetry up to rank $N = 12$.

$$\hat{\mathbf{Y}}^C_4(\theta,\phi) = \tfrac{1}{2}\sqrt{\tfrac{7}{3}}\mathbf{Y}^C_4(\theta,\phi)$$
$$\hat{\mathbf{Y}}^C_6(\theta,\phi) = \tfrac{1}{2\sqrt{2}}\mathbf{Y}^C_6(\theta,\phi)$$
$$\hat{\mathbf{Y}}^C_8(\theta,\phi) = \tfrac{\sqrt{33}}{8}\mathbf{Y}^C_8(\theta,\phi)$$
$$\hat{\mathbf{Y}}^C_{10}(\theta,\phi) = \tfrac{1}{8}\sqrt{\tfrac{65}{6}}\mathbf{Y}^C_{10}(\theta,\phi)$$
$$\hat{\mathbf{Y}}^C_{12}(\theta,\phi) = \tfrac{9}{20}\sqrt{\tfrac{11}{41}}\mathbf{Y}^C_{12}(\theta,\phi)$$

orthogonal, they are not normalized. A normalized set $\hat{\mathbf{Y}}^C_N$, and some of their properties, can be seen in tables 1b and 1c, respectively. For example if $\tilde{K}_4(T)$ is positive, the direction of easy magnetization lies along a ⟨111⟩ axis.

In passing we note that the multi-polar approach embodied in equation (3) possesses many advantages over the older phenomenological approach. In particular, the combinations of direction cosines in equations (1) and (2) do not represent a basis set. Indeed, it is this feature which is responsible for the bizarre changes of sign in the anisotropy parameters K_1 in $HoFe_2$ and K_2 in $DyFe_2$ found by A&D. By way of contrast, Martin *et al* (2006) showed that all the $\tilde{K}_n(T)$ parameters decay monotonically with increasing temperature, in accord with the original C&C model of magnetic anisotropy.

In summary, symmetry adapted harmonic sets are the natural way of expressing the magnetic anisotropy for all magnetic compounds. But before leaving this section, it is probably worth remarking that the same information can be extracted from quantum mechanical calculations, starting from the crystal field Hamiltonian $\mathcal{H}_{CF}$ acting on the RE^{3+} ions. This involves just two crystal field parameters B_4 and B_6, plus the spin J of the RE (see A&D for details). However this procedure is excessively time consuming, requiring repeated diagonalization of $(2J+1)\times(2J+1)$ matrices. In practice, it is mandatory to use the classical form of the magnetic anisotropy when modelling the properties of magnetic exchange spring $REFe_2/YFe_2$ systems, (Sawicki *et al* 2000, Dumesnil *et al* 2000, Bowden *et al* 2003, 2008).

In summary, the multi-polar expression for the anisotropy energy of equation (3) can be viewed as the *classical manifestation* of the Hamiltonian acting on the RE^{3+} ion in question. This, of course, is what is measured during a magnetic anisotropy experiment.

2. MBE grown films: rotation of the coordinate system

While tables 1a, 1b and 1c are suitable for the free-standing $REFe_2$ compounds, they are not, *a priori*, a suitable choice for multi-layer films grown by molecular beam epitaxy (MBE). The situation for (110) MBE films can be seen in figure 2. It will be observed that both the cubic x and y axes of the unit cell point out of the film plane at 45°.

The situation is different for the (111) MBE grown films, summarized in figure 3. Note that there is three-fold symmetry about the z-axis, as expected.

In both cases therefore, it is advantageous to adopt a new frame of reference where the z-axis is aligned along either the [110] or [111] growth axis. For the (110) films, this can be achieved using the Euler rotations $\alpha = \pi/4$, $\beta = \pi/2$, $\gamma = 0$, with the α rotation performed first. Specifically, for a given spherical harmonic:

$$Y^m_n(\theta,\phi) \rightarrow \sum_{m'} D^n_{m',m}(\alpha\beta\gamma)Y^{m'}_n(\theta,\phi)$$
$$= \sum_{m'} \mathrm{e}^{+\mathrm{i}m\pi/4} d^n_{m',m}(\beta=\pi/2)Y^{m'}_n(\theta,\phi) \qquad (4)$$

e.g. Edmonds (1960), Varshalovich *et al* (1989). Proceeding according to equation (4) therefore, it can be shown that the cubic harmonic combinations listed in tables 1a, 1b and 1c transform according to table 2.

However for the (111) MBE films, it is more convenient to adopt a frame of reference shown in figure 3. This can be achieved by setting the Euler rotations: $\alpha = \pi/4$, $\beta = \cos^{-1}(\sqrt{1/3})$. These rotations leave the new z-axis aligned along the [111] axis, at right angles to the film, with the y-axis still along the in-plane [$\bar{1}$10] cubic axis. However the new x-axis now points along a [11$\bar{2}$] direction. The results of this rotation are summarized in table 3.

Table 1c. Some properties of the spherical harmonics $\mathbf{Y}_N^C(\theta,\phi)$ with cubic symmetry up to rank $N = 12$.

	N_N	Min	θ (deg)	ϕ (deg)	Max	θ	ϕ
$\mathbf{Y}_4^C(\theta,\phi)$	$\frac{1}{2}\sqrt{\frac{7}{3}}$	$-\frac{1}{\sqrt{\pi}}$	54.7356	45	$\frac{1}{2}\sqrt{\frac{9}{\pi}}$	0	In det.
$\mathbf{Y}_6^C(\theta,\phi)$	$\frac{1}{2\sqrt{2}}$	$-\frac{13}{16}\sqrt{\frac{13}{\pi}}$	45	0	$\frac{1}{2}\sqrt{\frac{13}{\pi}}$	0	In det.
$\mathbf{Y}_8^C(\theta,\phi)$	$\frac{\sqrt{33}}{8}$	−0.702 52	27.7903	45	$\frac{1}{2}\sqrt{\frac{17}{\pi}}$	0	In det.
$\mathbf{Y}_{10}^C(\theta,\phi)$	$\frac{1}{8}\sqrt{\frac{65}{6}}$	−1.321 24	25.0411	0	$\frac{1}{2}\sqrt{\frac{21}{\pi}}$	0	In det.
$\mathbf{Y}_{12}^C(\theta,\phi)$	$\frac{9}{20}\sqrt{\frac{11}{41}}$	−3.8363	47.6665	23.2349	$\frac{1}{2}\sqrt{\frac{25}{\pi}}$	0	In det

Table 2. For this table the new (x, y, z)-axes coincide with the $[00\bar{1}]$, $[\bar{1}10]$, and $[110]$ directions. Here Y_n^m is a shorthand notation for $Y_n^m(\theta,\phi)$, and $Y_n^m(s,a)$ is a shorthand notation for $Y_n^m(\theta,\phi) \pm Y_n^{-m}(\theta,\phi)$, respectively.

$$\mathbf{Y}_4^C(\theta,\phi) \to [-\tfrac{1}{4}Y_4^0 - \tfrac{1}{2}\sqrt{\tfrac{5}{2}}Y_4^2(s) + \tfrac{3}{4}\sqrt{\tfrac{5}{14}}Y_4^4(s)]$$
$$\mathbf{Y}_6^C(\theta,\phi) \to [-\tfrac{13}{8}Y_6^0 + \tfrac{\sqrt{105}}{16}Y_6^2(s) + \tfrac{5}{8}\sqrt{\tfrac{7}{2}}Y_6^4(s) + \tfrac{\sqrt{231}}{16}Y_6^6(s)]$$
$$\mathbf{Y}_8^C(\theta,\phi) \to [\tfrac{9}{16}Y_8^0 + \tfrac{\sqrt{35}}{24}Y_8^2(s) + \tfrac{25}{24}\sqrt{\tfrac{7}{22}}Y_8^4(s) - \tfrac{7}{8}\sqrt{\tfrac{13}{33}}Y_8^6(s) + \tfrac{3}{16}\sqrt{\tfrac{65}{22}}Y_8^8(s)]$$
$$\mathbf{Y}_{10}^C(\theta,\phi) \to [-\tfrac{1}{32}Y_{10}^0 + \tfrac{13}{32}\sqrt{\tfrac{33}{10}}Y_{10}^2(s) - \tfrac{31}{16}\sqrt{\tfrac{33}{130}}Y_{10}^4(s) - \tfrac{83}{64}\sqrt{\tfrac{33}{65}}Y_{10}^6(s) + \tfrac{1}{32}\sqrt{\tfrac{187}{130}}Y_{10}^8(s) + \tfrac{3}{64}\sqrt{\tfrac{3553}{13}}Y_{10}^{10}(s)]$$
$$\mathbf{Y}_{12}^C(\theta,\phi) \to [\tfrac{839}{384}Y_{12}^0 - \tfrac{155}{192}\sqrt{\tfrac{91}{66}}Y_{12}^2(s) - \tfrac{785}{2304}\sqrt{\tfrac{91}{11}}Y_{12}^4(s) + \tfrac{49}{384}\sqrt{\tfrac{221}{11}}Y_{12}^6(s) + \tfrac{65}{384}\sqrt{\tfrac{4199}{66}}Y_{12}^8(s) + \tfrac{5}{384}\sqrt{\tfrac{29393}{3}}Y_{12}^{10}(s) + \tfrac{\sqrt{676039}}{768}Y_{12}^{12}(s)]$$

Table 3. For this table the new (x, y, z)-axes coincide with the $[11\bar{2}]$, $[\bar{1}10]$,and $[111]$ directions. See table 2 for abbreviations.

$$\mathbf{Y}_4^C(\theta,\phi) \to [-\tfrac{2}{3}Y_4^0 + \tfrac{2}{3}\sqrt{\tfrac{10}{7}}Y_4^3(a)]$$
$$\mathbf{Y}_6^C(\theta,\phi) \to [+\tfrac{16}{9}Y_6^0 + \tfrac{2}{9}\sqrt{\tfrac{70}{3}}Y_6^3(a) + \tfrac{2}{9}\sqrt{\tfrac{77}{3}}Y_6^6(s)]$$
$$\mathbf{Y}_8^C(\theta,\phi) \to [\tfrac{8}{27}Y_8^0 - \tfrac{16}{27}\sqrt{\tfrac{35}{33}}Y_8^3(a) + \tfrac{32}{27}\sqrt{\tfrac{13}{33}}Y_8^6(s)]$$
$$\mathbf{Y}_{10}^C(\theta,\phi) \to [-\tfrac{128}{81}Y_{10}^0 + \tfrac{16}{27}\sqrt{\tfrac{22}{195}}Y_{10}^3(a) + \tfrac{88}{27}\sqrt{\tfrac{11}{195}}Y_{10}^6(s) + \tfrac{8}{81}\sqrt{\tfrac{7106}{65}}Y_{10}^9(a)]$$
$$\mathbf{Y}_{12}^C(\theta,\phi) \to [\tfrac{3812}{2187}Y_{12}^0 + \tfrac{940}{2187}\sqrt{\tfrac{182}{11}}Y_{12}^3(a) + \tfrac{592}{2187}\sqrt{\tfrac{221}{11}}Y_{12}^6(s) + \tfrac{40}{2187}\sqrt{\tfrac{29393}{11}}Y_{12}^9(a) + \tfrac{4\sqrt{676039}}{2187}Y_{12}^{12}(s)]$$

In summary therefore, tables (2) and (3) summarize the magnetic anisotropy sets for the two MBE grown films in question. Finally, we remark that it would be very difficult to establish the rotational properties of phenomenological form of the magnetic anisotropy (see equations (1) and (2) above).

3. The magneto-elastic Hamiltonian

So far the results given above only apply to the free-standing $REFe_2$ compounds. However, in the case of (110) MBE grown crystals it is known that as the crystal cools down, the $REFe_2$ film shrinks more than the underlying sapphire substrate. This differential contraction gives rise to strain components $\varepsilon_{xx}, \varepsilon_{xy}$ etc. For example in (110) MBE grown films, the dominant strain component is the shear term $\varepsilon_{xy} \sim -0.05$ (Mougin *et al* 2000). This term gives rise to an additional rank 2 magneto-crystalline anisotropy which favours out-of-plane magnetization for $ErFe_2$, and in-plane magnetization for $DyFe_2$. The strain components for (111) MBE films have yet to be measured. However, we speculate (see below) that the important strain components will be the three shear terms $\varepsilon_{xy} = \varepsilon_{yz} = \varepsilon_{xz} \approx -0.05$. On this basis, it is possible to make some predictions for the five $REFe_2$ (111) MBE films, with RE = Tb, Dy, Ho, Er and Tm.

The general magneto-elastic Hamiltonian can be written in the form:

$$\mathcal{H}_{\mathrm{ME}} = b_2\varepsilon_{xx}\alpha_x^2 + b_2\varepsilon_{yy}\alpha_y^2 + b_2\varepsilon_{zz}\alpha_z^2 + b_2\varepsilon_{xy}\alpha_x\alpha_y + b_2\varepsilon_{xz}\alpha_x\alpha_z + b_2\varepsilon_{yz}\alpha_y\alpha_z. \quad (5)$$

Following Hutchings (1964), Abragam and Bleaney (1970) and Bowden *et al* (2006), equation (5) is transformed to:

$$\mathcal{H}_{\mathrm{ME}} = B_{xx}\mathbf{J}_x^2 + B_{yy}\mathbf{J}_y^2 + B_{zz}\mathbf{J}_z^2 + B_{xy}\tfrac{1}{2}\left(\mathbf{J}_x\mathbf{J}_y + \mathbf{J}_y\mathbf{J}_x\right) + B_{xz}\tfrac{1}{2}\left(\mathbf{J}_x\mathbf{J}_z + \mathbf{J}_z\mathbf{J}_x\right) + B_{yz}\tfrac{1}{2}\left(\mathbf{J}_y\mathbf{J}_z + \mathbf{J}_z\mathbf{J}_y\right) \quad (6)$$

where:

$$B_{ij} = \left[\frac{b_2\varepsilon_{ij}}{J(J+1)}\right]. \quad (7)$$

However, in place of the spin operators $\mathbf{J}_\alpha$, we choose to use the tensor operators $\mathbf{T}_q^k$, which obey the same transformation laws as the spherical harmonics of equation (4) (see Bowden and Hutchison 1986, Martin *et al* 2006). Equation (6) therefore takes the form:

$$\mathcal{H}_{\mathrm{ME}} = B_{xx}\left\{\tfrac{1}{2}\left[\mathbf{T}_2^2 + \mathbf{T}_{-2}^2\right] - \tfrac{1}{2}\left[\sqrt{\tfrac{2}{3}}\mathbf{T}_0^2 - \tfrac{2}{3}J(J+1)\right]\right\} + B_{yy}\left\{-\tfrac{1}{2}\left[\mathbf{T}_2^2 + \mathbf{T}_{-2}^2\right] - \tfrac{1}{2}\left[\sqrt{\tfrac{2}{3}}\mathbf{T}_0^2 - \tfrac{2}{3}J(J+1)\right]\right\}$$

Table 4. The spherical harmonic combinations for a general strain with respect to the free-standing Laves phase compounds.

Distortion	Angular form
ε_{xx}	$(Y_2^2(s) - \sqrt{\frac{3}{2}}Y_2^0) =$ $\eta(\sin^2\theta\cos 2\phi - \frac{1}{2\sqrt{2}}(3\cos^2\theta - 1))$
ε_{yy}	$-(Y_2^2(s) + \sqrt{\frac{3}{2}}Y_2^0) =$ $-\eta(\sin^2\theta\cos 2\phi + \frac{1}{2\sqrt{2}}(3\cos^2\theta - 1))$
ε_{zz}	$2\sqrt{\frac{2}{3}}Y_2^0 = \eta\frac{2}{3}(3\cos^2\theta - 1)$
ε_{xy}	$-\mathrm{i}Y_2^2(a) = \eta\sin^2\theta\sin 2\phi$
ε_{yz}	$-Y_2^1(a) = \eta\sin 2\theta\cos\phi$
ε_{xz}	$+\mathrm{i}Y_2^1(s) = \eta\sin 2\theta\sin\phi(\eta = \frac{1}{2}\sqrt{\frac{15}{2\pi}})$

$$+ B_{zz}\left\{\left[\sqrt{\frac{2}{3}}\mathbf{T}_0^2 + \frac{1}{3}J(J+1)\right]\right\} - B_{xy}\frac{\mathrm{i}}{2}\left[\mathbf{T}_2^2 - \mathbf{T}_{-2}^2\right] - \frac{1}{2}B_{xz}\left[\mathbf{T}_1^2 - \mathbf{T}_{-1}^2\right] + B_{yz}\frac{\mathrm{i}}{2}\left[\mathbf{T}_1^2 + \mathbf{T}_{-1}^2\right]. \quad (8)$$

In the (110) MBE films, the dominant distortion is the shear term ε_{xy} (Mougin *et al* 2000). Consequently:

$$\mathcal{H}_{\mathrm{ME}}(\varepsilon_{xy}) = -B_{xy}\frac{\mathrm{i}}{2}\left[\mathbf{T}_2^2 - \mathbf{T}_{-2}^2\right]. \quad (9)$$

However in [111] MBE grown films, we believe that the three shear terms $\varepsilon_{xy}, \varepsilon_{xy}, \varepsilon_{xy}$ will be almost equal and dominant. Thus:

$$\mathcal{H}_{\mathrm{ME}}(\varepsilon_{xy}) = -B_{xy}\frac{\mathrm{i}}{2}\left[\mathbf{T}_2^2 - \mathbf{T}_{-2}^2\right] - \frac{1}{2}B_{xz}\left[\mathbf{T}_1^2 - \mathbf{T}_{-1}^2\right] + B_{yz}\frac{\mathrm{i}}{2}\left[\mathbf{T}_1^2 + \mathbf{T}_{-1}^2\right]. \quad (10)$$

Nonetheless, in order to cover all possibilities, the additional magnetic anisotropy for a general distortion is fully delineated in section 4.

4. First order magnetic anisotropy terms for a general distortion

Following Callen and Callen (1965, 1966) and Callen and Shtrikman (1965), the first order change in the free energy due to a general distortion takes the form:

$$F' = \langle\mathcal{H}_{\mathrm{ME}}\rangle = \sum_{n,m}\tilde{B}_m^n\mathcal{D}_{0m}^n(\omega)\left\langle T_0^n\right\rangle$$
$$= \tilde{K}'_{xx}\left[\left(Y_2^2(\theta,\phi) + Y_2^{-2}(\theta,\phi)\right) - \sqrt{\tfrac{2}{3}}Y_2^0(\theta,\phi)\right] + \tilde{K}'_{yy}\left[-\left(Y_2^2(\theta,\phi) + Y_2^{-2}(\theta,\phi)\right) - \sqrt{\tfrac{2}{3}}Y_2^0(\theta,\phi)\right] + \tilde{K}'_{zz}\left[2\sqrt{\tfrac{2}{3}}Y_2^0(\theta,\phi)\right] + \tilde{K}'_{xy}\mathrm{i}[Y_2^{-2}(\theta,\phi) - Y_2^2(\theta,\phi)] + \tilde{K}'_{xz}\left[Y_2^{-1}(\theta,\phi) - Y_2^1(\theta,\phi)\right] + \tilde{K}'_{zy}\mathrm{i}\left[Y_2^1(\theta,\phi) + Y_2^{-1}(\theta,\phi)\right]. \quad (11)$$

Here the anisotropy parameters are given by:

$$\tilde{K}'_{ij} = \sqrt{\frac{\pi}{5}}B_{ij}\left\langle T_0^2\right\rangle_{EX} \qquad (i,j = x,y,z). \quad (12)$$

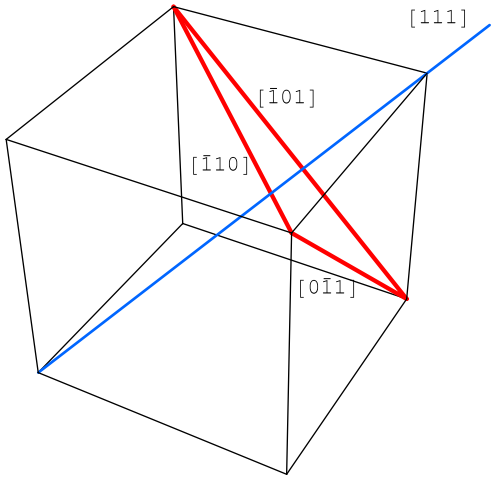

Figure 4. The $REFe_2$ Laves unit cell relative to the plane of the (111) MBE grown film.

Note that (i) the combinations of spherical harmonics appearing in equation (11) are real, and (ii) every distortion scales with temperature according to $\langle\mathbf{T}_0^2\rangle_{EX}$, in accord with the original C&C model of anisotropy. For convenience, the spherical harmonic combinations appearing in equation (11) are summarized in table 4.

Using equations (4) and (11) it is relatively straightforward to calculate the new angular forms for the three geometries under question. The results are summarized in table 5. Note that for the distortion proposed in this paper for the (111) MBE grown films, the angular form of the distortion reduces to $\sqrt{6}Y_2^0(\theta,\phi)$, as expected.

In summary, all the information required by a modeller of $REFe_2/YFe_2$ magnetic exchange springs is summarized in tables (1a–5). In fact, it was the need for such tables that provided one of the major motivations behind this work. Taken together, with the multi-polar anisotropy parameters $\tilde{K}_4(T)$ etc, of Martin *et al* (2006), and strain parameters $\tilde{K}_{xy}(T)$ etc, of Bowden *et al* (2006), the modeller has all the I/P parameters required both for free standing and (110) and (111) MBE grown $REFe_2$ films.

5. Directions of preferred magnetization in the (111) MBE grown MBE films

As mentioned earlier, no x-ray results detailing the distortions in (111) MBE films are currently available. Nevertheless it is possible to make progress as follows.

The principle cubic axes can be seen in figure 4. Note the plane defined by the face diagonals [$\bar{1}$01], [$\bar{1}$10], and [0$\bar{1}$1] (red on-line) lie in the plane of the film, at right angles to [111] growth axis (blue on-line).

As the MBE grown film cools down, the $REFe_2$ film will be stretched in the plane of the film. Presumably this will be accompanied by a decrease in the [111] direction, as the film tries to conserve volume. However the *new* [$\bar{1}$01], [$\bar{1}$10], and [0$\bar{1}$1] axes will still be confined to the plane of the film at right angles to the [111] direction. This information can be used to partially unravel the distortions that can occur.

Table 5. Angular forms for the six components of the shear strain tensor $\boldsymbol{\varepsilon}$, referred to (a) the free-standing material with z-axis aligned with the cubic [001] axis, (b) (110)-grown MBE films with the z-axis parallel to the [110] axis, and (c) (111) grown MBE films with the z-axis parallel to the [111] axis. See table 2 for abbreviations.

	$z \parallel^{rl}$ [001]	$z \parallel^{rl}$ [110]	$z \parallel^{rl}$ [111]
ε_{xx}	$-\sqrt{\frac{2}{3}}Y_2^0 + Y_2^2(s)$	$\frac{1}{\sqrt{6}}Y_2^0 - \mathrm{i}Y_2^1(s) - \frac{1}{2}Y_2^2(s)$	$\{-\mathrm{i}\sqrt{\frac{2}{3}}Y_2^1(s) - \frac{\sqrt{2}}{3}Y_2^1(a) - \frac{1}{3}Y_2^2(s) + \frac{\mathrm{i}}{\sqrt{3}}Y_2^2(a)\}$
ε_{yy}	$-\sqrt{\frac{2}{3}}Y_2^0 - Y_2^2(s)$	$\frac{1}{\sqrt{6}}Y_2^0 + \mathrm{i}Y_2^1(s) - \frac{1}{2}Y_2^2(s)$	$\{+\mathrm{i}\sqrt{\frac{2}{3}}Y_2^1(s) - \frac{\sqrt{2}}{3}Y_2^1(a) - \frac{1}{3}Y_2^2(s) - \frac{\mathrm{i}}{\sqrt{3}}Y_2^2(a)\}$
ε_{zz}	$2\sqrt{\frac{2}{3}}Y_2^0$	$-\sqrt{\frac{2}{3}}Y_2^0 + Y_2^2(s)$	$\frac{2\sqrt{2}}{3}Y_2^1(a) + \frac{2}{3}Y_2^2(s)$
ε_{xy}	$-\mathrm{i}Y_2^2(a)$	$\sqrt{\frac{3}{2}}Y_2^0 + \frac{1}{2}Y_2^2(s)$	$\sqrt{\frac{2}{3}}Y_2^0 - \frac{\sqrt{2}}{3}Y_2^1(a) + \frac{2}{3}Y_2^2(s)$
ε_{xz}	$-Y_2^1(a)$	$\frac{1}{\sqrt{2}}Y_2^1(a) - \mathrm{i}\frac{1}{\sqrt{2}}Y_2^2(a)$	$\{\sqrt{\frac{2}{3}}Y_2^0 + \frac{1}{3\sqrt{2}}Y_2^1(a) - \frac{\mathrm{i}}{\sqrt{6}}Y_2^1(s) - \frac{1}{3}Y_2^2(s) - \frac{\mathrm{i}}{\sqrt{3}}Y_2^2(a)\}$
ε_{yz}	$\mathrm{i}Y_2^1(s)$	$\frac{1}{\sqrt{2}}Y_2^1(a) + \mathrm{i}\frac{1}{\sqrt{2}}Y_2^2(a)$	$\{\sqrt{\frac{2}{3}}Y_2^0 + \frac{1}{3\sqrt{2}}Y_2^1(a) + \frac{\mathrm{i}}{\sqrt{6}}Y_2^1(s) - \frac{1}{3}Y_2^2(s) + \frac{\mathrm{i}}{\sqrt{3}}Y_2^2(a)\}$

Table 6. Strain-induced magneto-elastic parameters in (111) MBE grown films, together with predictions for strain-induced directions of easy magnetization, and those of the bulk compounds (taken from Bowden *et al* 1968).

	b_2 (J m^{-3})	b_2 (K/ion)	B_{xy} (K/ion)	Easy-axis (Strain)	Easy-axis (Cubic)
Tb	-6.41×10^8	-2.29×10^3	0.300	In-plane	⟨111⟩
Dy	-6.11×10^8	-2.17×10^3	0.187	In-plane	⟨001⟩
Ho	-2.33×10^8	-0.84×10^3	0.071	In-plane	⟨001⟩
Er	$+2.19 \times 10^8$	$+0.76 \times 10^3$	-0.066	Out-of-plane [111]	⟨111⟩
Tm	$+5.39 \times 10^8$	$+1.92 \times 10^3$	-0.242	Out-of-plane [111]	⟨111⟩

If the new face diagonals $[\bar{1}01]$, $[\bar{1}10]$, and $[0\bar{1}1]$ are at right angles to the [111] direction, it is easy to show that:

$$\begin{aligned}(\varepsilon_{zz} - \varepsilon_{xy}) + (\varepsilon_{xz} - \varepsilon_{yy}) &= 0\\ (\varepsilon_{zz} - \varepsilon_{xy}) + (\varepsilon_{yz} - \varepsilon_{xx}) &= 0\\ (\varepsilon_{xx} - \varepsilon_{yz}) + (\varepsilon_{xz} - \varepsilon_{yy}) &= 0.\end{aligned} \tag{13}$$

One solution which conserves volume to second order is given by:

$$\begin{aligned}\varepsilon_{xx} = \varepsilon_{yy} = \varepsilon_{zz} &= 0\\ \varepsilon_{xy} = \varepsilon_{xz} = \varepsilon_{yz} &= -\varepsilon.\end{aligned} \tag{14}$$

With this particular solution the new length of the three face diagonals is given by $\sqrt{2}a_o(1+\varepsilon)$ i.e. an expansion, while the body diagonal shrinks to $\sqrt{3}a_o(1-2\varepsilon)$. If we set $\varepsilon = -0.05$ we find the values of B_{xy} etc, set out in table 6. This table can be compared with table II of Mougin *et al* (2000) and table II of Bowden *et al* (2006), for the (110) MBE films.

Note that the $ErFe_2$ and $TmFe_2$ (111) films are unique in that both the cubic (bulk) and strain-induced anisotropies favour out of plane magnetization, along the [111] growth axis. Recent magnetic measurements on $ErFe_2$ (111) films and neutron-reflectometry measurements support this conclusion (Rainford *et al* 2008).

Finally, it should be mentioned that the three in-plane face diagonals shown in figure 4, lie in the $(11\bar{2}0)$ plane of the sapphire substrate. Consequently, if the thermal contraction of the sapphire in this plane (essentially c–a) is uniform, the conclusion reached above, namely $\varepsilon_{xy} = \varepsilon_{xz} = \varepsilon_{yz} = -\varepsilon$ at room temperature is valid. However Lucht *et al* (2003) have shown that for $T > 200$ K the linear coefficients of expansion are $\alpha_a = 6.2(2) \times 10^{-6}$ K^{-1} and $\alpha_C = 7.07(8) \times 10^{-6}$ K^{-1}. Thus a small difference in the contraction of the three face diagonals in figure 3 can be anticipated. At lower temperatures $T < 200$ K, nonlinear behaviour will occur. Clearly precise x-ray measurements will be required for a definitive exposition of the effect of strain on the magnetic properties of (111) MBE grown films. For the present therefore, table 6 must serve as a first approximation.

6. Conclusions

In this paper, symmetry adapted harmonic sets have been set out for the Laves phase $REFe_2$ compounds, both for free-standing compounds and MBE thin films grown in either the (110) or (111) mode. In addition, the general problem of induced distortions of the cubic lattice, for (110) and (111) MBE grown films has also been examined in some detail. The results have subsequently been used to make predictions concerning the strain-induced preferred direction of easy magnetization in (111) MBE grown films. In particular it has been argued that both $TmFe_2$ and $ErFe_2$ are unique, in that both the bulk crystalline magneto-crystalline anisotropy and strain-induced anisotropy favour out of plane magnetization.

Acknowledgments

We would like to acknowledge EPSRC grant No. GR/S95824, under which this work was performed.

One of us (GJB) would like to acknowledge a useful conversation with Glen Stewart of University College, ADFA, Canberra.

References

Abragam A and Bleaney B 1970 *Electron Paramagnetic Resonance of Transition Ions* (Oxford: Clarendon)

Atzmony U and Dariel M P 1976 *Phys. Rev.* B **13** 4006–14

Atzmony U, Dariel M P, Bauminger E R, Lebenbaum D, Nowik I and Ofer S 1973 *Phys. Rev.* B **7** 4220–32
Bowden G J, Beaujour J-M L, Zhukov A A, Rainford B D, de Groot P A J, Ward R C C and Wells M R 2003 *J. Appl. Phys.* **93** 6480–2
Bowden G J, Bunbury D St P, Guimaraes A P and Synder R E 1968 *J. Phys. C: Solid State Phys.* **1** 1376
Bowden G J, de Groot P A J, Rainford B D, Wang K, Martin K N, Zimmermann J P and Fangohr H 2006 *J. Phys.: Condens. Matter* **18** 5861–71
Bowden G J and Hutchison W D 1986 *J. Magn. Reson.* **67** 403–15
Bowden G J, Martin K N, Rainford B D and de Groot P A J 2008 *J. Phys.: Condens. Matter* **20** 015209
Bozorth R M 1961 *Ferromagnetism* (New York: Van Nostrand)
Callen H B and Callen E 1965 *J. Phys. Rev.* **139** A455–71
Callen H B and Callen E 1966 *J. Phys. Chem. Solids* **27** 1271–85
Callen H B and Shtrikman S 1965 *Solid State Commun.* **3** 5–8
Coey J M D and Skomski R 1993 *Phys. Scr.* T **49** 315
Dumesnil M, Dutheil M, Dufour C and Mangin Ph 2000 *Phys. Rev.* B **62** 1136
Edmonds A R 1960 *Angular Momentum in Quantum Mechanics* (Princeton, NJ: Princeton University Press)
Hutchings M T 1964 *Solid State Phys.* vol 16 (New York: Academic) p 227
Lucht M, Lerche M, Wille H-C, Shvyd'ko Yu V, Rüter H D, Gerdau E and Becker P 2003 *J. Appl. Crystallogr.* **36** 1075
Martin K N, de Groot P A J, Rainford B D, Wang K, Bowden G J, Zimmermann J P and Fangohr H 2006 *J. Phys.: Condens. Matter* **18** 459–78
Martin K N *et al* 2008 at press
Mougin A, Dufour C, Dumesnil K and Mangin Ph 2000 *Phys. Rev.* B **62** 9517–31
Rainford B D *et al* 2008 at press
Sawicki M, Bowden G J, de Groot P A J, Rainford B D, Beaujour J-M L, Ward R C C and Wells M R 2000 *Phys. Rev.* B **62** 5817
Varshalovich D A, Moskalev A N and Khersonskii V K 1989 *Quantum Theory of Angular Momentum* (Singapore: World Scientific)